REPORT SERIES IN AEROSOL SCIENCE
N:o 218 (2019)

DEVELOPING METHODS FOR DOPPLER LIDAR TO INVESTIGATE ATMOSPHERIC BOUNDARY LAYER

ANTTI JUHANI MANNINEN

Institute for Atmospheric and Earth System Research / Physics
Faculty of Science
University of Helsinki
Helsinki, Finland

Academic dissertation

To be presented, with the permission of the Faculty of Science of the University of Helsinki, for public criticism in auditorium A110, Chemicum, A. I.Virtasen aukio 1, on May 10th, 2019, at 12 o'clock noon.

Helsinki 2019

Author's Address: Institute for Atmospheric and Earth System Research / Physics
P.O. Box 64
FI-00014 University of Helsinki
e-mail antti.j.manninen@helsinki.fi

Supervisors: Professor Tuukka Petäjä, Ph.D.
Department of Physics
University of Helsinki, Finland

Tenure-track Professor Ewan O'Connor, Ph.D.
Finnish Meteorological Institute, Helsinki,
University of Reading, UK

Reviewers: Professor Janet Barlow, Ph.D.
Department of Meteorology
University of Reading, UK

Assistant Professor Siegfried Schobesberger, Ph.D.
Department of Applied Physics
University of Eastern Finland

Opponent: Professor Lucas Alados Arboledas, Ph.D.
Applied Physics Department
University of Granada, Spain

ISBN 978-952-7276-18-1 (printed version)
Helsinki 2019
Unigrafia Oy

ISBN 978-952-7276-19-8 (pdf version)
http://www.atm.helsinki.fi/FAAR/
Helsinki 2019

Acknowledgements

The research for this thesis was carried out at the Institute for Atmospheric and Earth System Research / Physics, University of Helsinki. I thank the former head of the department, Prof. Hannu Koskinen for providing me with the facilities for this work. I want to sincerely thank the head of the INAR, Prof. Markku Kulmala for giving me the opportunity to work at the division in the beginning. Also, I am most grateful for Prof. Tuukka Petj for supervising my PhD thesis, for taking me into BAECC project when I started my PhD studies, and for always having time for any questions I might've had. I express my sincere gratitude to tenure-track Prof. Ewan O'Connor from the Finnish Meteorological Institute for supervising my PhD thesis, guiding me in my research and in scientific writing, and for introducing me to the European community of researchers from our field.

Since academia was almost completely new environment for me, I wish to sincerely thank Dr. Ville Vakkari from the Finnish Meteorological Institute for giving me valuable advice especially in the beginning of my PhD studies. I equally appreciate Tobias Marke from the University of Cologne for the relentless effort over several years to develop our boundary layer classification scheme and for his persistence to get the paper about the topic to get written. I am most grateful for Anna Franck and Ksenia Tabakova for being the most kind and friendly office mates I could ask for and with whom I could always exchange ideas. The most exciting research projects I worked for during my PhD studies was the Cessna flight campaigns. Aside from having had the chance to sit in a small and cramped airplane while admiring the magical view of homogeneous boreal forest in every direction, this was the only project where I got the chance to work outside the office. I sincerely thank Dr. Riikka Väänänen, Katri Leino, and Janne Lampilahti for organising these campaigns and allowing me to participate year after year.

I thank my friends Andac, Elina, Juho, Lassi, Lauri, Markus, Mikko K., Mikko S., and Teppo for the long–lasting friendship. I would like to thank my parents for supporting me in my studies from the beginning to the end and especially during the years I studied abroad. Equally, I would like to thank Juha for shaking loose my occasional ingrained thoughts and first and foremost being an excellent brother. Finally, I would like to sincerely thank Vilma since without you I might've buckled under the stress while finishing my thesis and while preparing for the defence. Your support made me feel calm and confident about the whole thing.

Antti Juhani Manninen
University of Helsinki, 2019

Abstract

Global and in–situ wind field observations are crucial for predicting weather and climate. Air motions and turbulence within the part of the Earth's atmosphere, which is influenced by the surface and called the atmospheric boundary layer (ABL), affect aerosol–cloud interactions and are essential in forecasting poor air quality episodes. During the last few decades remote sensing instruments, especially Doppler lidars, have been shown to be able to monitor the vertical profile of the ABL with very high time and height resolution. Doppler lidars can measure the vertical velocity directly in vertical pointing mode and with a scanning capability also retrieve the horizontal winds. Further, from Doppler lidar measurements profiles of estimated turbulent properties, wind shear, and higher order velocity statistics, such as skewness and kurtosis, can be calculated, which can be used to reveal detailed information on the ABL vertical structure.

Pulsed Doppler lidar systems using heterodyne detection usually operate in the near–infrared spectral region. They transmit a laser pulse which scatters from atmospheric particles, mostly aerosols, and the backscattered part is recorded by the instruments. There are significant limitations in the sensitivity of pulsed Doppler lidar systems in locations where aerosol load is low and hence the signal–to–noise ratio (SNR) is low. In theory, sensitivity of a pulsed Doppler lidar system discussed in this thesis can be improved by averaging the signal, which increases the SNR assuming the noise is Gaussian. If the noise is not Gaussian the improvement in sensitivity is effectively limited by the noise characteristics. Also, any bias in the SNR is propagated into the vertical velocity uncertainties and thus to estimations of turbulent properties.

This thesis is comprised of research which aimed to properly characterize the noise in the backscatter signal of a pulsed Doppler lidar system, and to develop methods for correcting any bias detected in the noise. The instrument's sensitivity was improved significantly which increased data availability and usability of the instrument in general. Method for classifying ABL turbulent mixing was developed as well by combining several Doppler lidars quantities. The classification method enables estimating the coupling of turbulence to the surface and/or clouds as well as identifying the sources causing turbulent mixing within the ABL. Data processing methods developed for correcting the bias in the backscatter signal of the Doppler lidar system were applied to detect elevated aerosol layers from measurements of another profiling lidar system. The developed methods were collected into a freely available software toolbox with the ultimate aim of generating harmonized Doppler lidar products across European Doppler lidar sites.

Keywords: Doppler lidar measurements, atmospheric boundary layer, data processing

Contents

List of publications

This thesis consists of an introductory review, followed by 5 research articles. In the introductory part, these papers are cited according to their roman numerals.

I **Manninen, A.J.**, O'Connor, E.J., Vakkari, V., Petäjä, T. (2016). A generalised background correction algorithm for a Halo Doppler lidar and its application to data from Finland, *Atmospheric Measurement Techniques*, 9(2):817–827, DOI:10.5194/amt-9-817-2016. Reproduced under Creative Commons Attribution License.

II Vakkari, V., **Manninen, A.J.**, O'Connor E.J., Schween J.H., van Zyl, P.G. (2019). A novel post-processing algorithm for Halo Doppler lidars, *Atmospheric Measurement Techniques*, DOI:10.5194/amt-12-839-2019. Reproduced under Creative Commons Attribution License.

III **Manninen, A.J.**, Marke T., Tuononen M., O'Connor, E.J. (2018). Atmospheric boundary layer classification with Doppler lidar, *Journal of Geophysical Research: Atmospheres*, 123(15):8172–8189, DOI:10.1029/2017JD028169. ©John Wiley and Sons. Used with permission.

IV Nikandrova, A., Takabova, K., **Manninen, A.J.**, Väänänen, R., Petäjä, T., Kulmala, M., Kerminen, V-M., O'Connor, E.J. (2018). Combining airborne in situ and ground-based lidar measurements for attribution of aerosol layers, *Atmospheric Chemistry and Physics*, 18(14):10575–10591, DOI:10.5194/acp-18-10575-2018. Reproduced under Creative Commons Attribution License.

V Petäjä, T., O'Connor, E.J., Moisseev, D., Sinclair V.A., **Manninen, A.J.**, Väänänen, R., von Lerber, A., Thornton, J. A., Nicoll, K., Petersen, W., Chandrasekar, V., Smith, J. N., Winkler, P. M., Krüger, O., Hakola, H., Timonen, H., Brus, D., Laurila, T., Asmi, E., Riekkola, M., Mona, L., Massoli, P., Engelmann, R., Komppula, M., Wang, J., Kuang, C., Bäck, J., Virtanen, A., Levula, J., Ritsche, M. and Hickmon, N. (2016), BAECC: A field campaign to elucidate the impact of biogenic aerosols on clouds and climate, *Bulletin of the American Meteorological Society*, 97(10):1909–1928, DOI:10.1175/BAMS-D-14-00199.1. ©American Meteorological Society. Used with permission.

1 Introduction

The World Meteorological Organisation (WMO) has determined that for high resolution numerical weather prediction (NWP) models wind speed and direction profiles are the most important but not yet adequately measured atmospheric parameter (World Meteorological Organization, 2018). The modest quality or at some areas the complete lack of observations of the wind field is specified to be the main limitation for improving these models. Also, the vertical wind component is considered as an important parameter, but the NWP model spatial resolution needs to be increased drastically before proper comparison with observations can be made.

To measure wind in the Earth's atmosphere, most remote sensing methods utilize the Doppler effect, i.e. Doppler shift. Pulsed Doppler lidars operate in the optical spectral region and can observe the wind component projected to the line–of–sight of the instrument, i.e. the radial velocity v (e.g. Reitebuch, 2012). Pulsed Doppler lidars emit a laser pulse, which propagates through the atmosphere at the speed of light c, scatters from atmospheric particles and molecules, and the backscattered part of the pulse is received and recorded by the instrument (e.g. Sonnenschein and Horrigan, 1971). If operating in the near–infrared spectral region the backscattered returns mainly originate from aerosols or cloud particles (Pearson et al., 2009), and scattering due to air molecules in the near–infrared is weak and negligible (Turner et al., 2016). Radial velocity can be obtained in terms of frequency by measuring the change between the emitted laser pulse frequency f_0 and the received backscattered part of the laser pulse frequency f (e.g. Werner et al., 2005), as given by:

$$v = c\,\Delta f\,\frac{1}{2f_0}, \tag{1}$$

where $\Delta f = f - f_0$ is the Doppler shift which, in turn, can be written as (Reitebuch, 2012):

$$\Delta f = 2\,f_0\,\frac{v}{c}. \tag{2}$$

Considering that the usual wind speeds within the Earth's atmosphere are in the order of 10^{-1}-10^{2} m s^{-1}, Doppler lidar operating in the near–infrared spectral region (1.5 µm) must be capable of detecting an extremely small Doppler shift which is in the order of 10^{6}-10^{9} Hz in terms of frequency or in the order of 10^{-15}-10^{-12} m in terms of wavelength. This sets very high challenges for the instrument. Thus many Doppler lidars systems

utilize the heterodyne technique where a local oscillator generates a reference signal at a constant frequency which is then mixed with the outgoing and incoming signal. The difference of the two is a low frequency signal which then can be accurately measured (Werner et al., 2005).

The pulsed Doppler lidars achieve eye–safe requirements with low–pulse energy and high pulse repetition rate (Pearson et al., 2009), but this affects the instrument sensitivity. Especially in clean–air locations, such as polar regions for instance, there are severe limitations in the performance of these type of Doppler lidars (e.g. **Paper I**). Clean–air refers to less atmospheric particles from which the emitted laser pulse can backscatter, lower signal–to–noise ratio (SNR), and hence reduced data availability (**Papers I-II**). Therefore, it is to be noted that in order to measure the radial velocities with acceptable uncertainties and use them further for scientific observations, the instrument needs to be characterized properly.

When pointing vertically, Doppler lidars can measure the vertical velocity directly with very high vertical and temporal resolutions (e.g. Hogan et al., 2009; Schween et al., 2014). This is very useful for investigating the lowest part of the troposphere, which is continuously or intermittently influenced by the surface and generally referred as the atmospheric boundary layer (ABL) (Stull, 1988; American Meteorological Society, 2019a). The part of the ABL, which is stirred by turbulence and where atmospheric gases, particles, temperature, and momentum are effectively mixed vertically and coupled with the surface and/or clouds, is termed the mixed layer (American Meteorological Society, 2019b). The height of this layer, i.e. mixed layer height (MLH), depends on the strength of turbulent mixing, which, in turn, is generated by buoyancy and/or wind shear (Moeng and Sullivan, 1994). When present, buoyancy driven turbulence is the most dominant source for mixing (Oke, 1992). Buoyancy is produced by surface heating which creates upward plumes of air, called updrafts, or by cloud–top radiative cooling which creates downdrafts (Garratt, 1994). The up– and downdrafts are clearly visible in the Doppler lidar vertical radial velocities and by calculating variance and skewness of the measured vertical velocities the source for the buoyancy generated turbulence can be estimated (Hogan et al. (2009); Harvey et al. (2013); **Paper III**). In general, the mixed layer grows when turbulent mixing increases and erodes when no turbulence is present (Oke, 1992); a process which can be continuously monitored by Doppler lidar (e.g. Schween et al., 2014).

Some Doppler lidars have also a scanning ability, which enables the retrieval of wind speed and direction profiles (Schwiesow et al., 1985; Grund et al., 2001), though horizontally homogeneous wind field has to be assumed (Päschke et al., 2015; Newsom et al., 2017). When scanning with a low elevation angle (the angle between the horizon and the line–of–sight), observations of low–level winds, wind shear, and low–level jets near the surface are also possible (e.g. Vakkari et al., 2015; Tuononen et al., 2017). Wind shear is generated when two layers of air are moving at different speeds and/or to different directions, or when a layer of air is moving over a stationary surface creating mechanical friction and turbulent mixing. The amount of turbulent mixing and how deep the mixing layer can grow depends on various factors: pre–existing atmospheric profile, the amount of solar radiation reaching the surface and thus the strength of the heat flux, wind speed, presence of clouds, and from meso- to synoptic-scale weather phenomena (e.g. Oke, 1992; Garratt, 1994).

In general, better understanding of the processes controlling and influencing the ABL remains essential for the NWP and climate models (Baklanov et al., 2011). Also, accurate and continuous representation of the whole ABL vertical structure is important for forecasting poor air quality episodes in dense urban environments (e.g. Anderson et al., 2012). The complexity of Earth's atmosphere sets high challenges, though. The ABL structure exhibits significant temporal and spatial variations (e.g. Deardorff, 1972), which makes measuring and numerical modeling the turbulent mixing and MLH accurately a very challenging task (Baklanov et al., 2011; Holtslag et al., 2013). The temporal and spatial scales involved with the turbulent mixing within the ABL are outside the scales which the models are able to represent (Cohen et al., 2015). Regardless, the models require accurate estimates of turbulent mixing within the ABL in order to predict local ABL flows reliably (Nielsen-Gammon et al., 2010). ABL parameterization schemes thus play an important part in decreasing the uncertainties of the model prediction and also long–term data sets depicting the vertical structure of the ABL are required (Baklanov and Grisogono, 2008; Harvey et al., 2015).

Doppler lidars can retrieve several atmospheric quantities with high temporal and vertical resolution, which can be combined to estimate turbulent coupling (Harvey et al., 2013) and to classify turbulence based on its source (**Paper III**), and further to develop ABL parameterization schemes (e.g. Harvey et al., 2015). Cataloguing climatologies generated from Doppler lidar quantities at various types of sites and environments different ABL types can be parameterized. Doppler lidar measurements provide also

an essential contribution for aerosol–cloud interaction studies when combined with an array of other remote sensing and in–situ observations (**Paper V**).

This thesis focused on improving the sensitivity, data availability and hence the usability of a pulsed heterodyne detection Doppler lidar system especially at high–latitude and other clean–air locations, and to develop site–independent methods for generating harmonized Doppler lidar products for cataloguing the ABL vertical structure. The main objectives for this thesis were:

i to characterize instrument performance and to improve data availability (**Paper I**),

ii to improve radial velocity uncertainties and enable robust estimate of turbulent properties (**Paper II**),

iii objective identification of the various sources of turbulent mixing (**Paper III**),

iv combine the developed methods into a software toolbox for processing Doppler lidar data (Manninen, 2019),

v and to apply data processing methodologies to different instrument types to investigate aerosol layers (**Paper IV**).

2 Methods

Robust measurement uncertainty estimates are vital for any noisy measurements. Atmospheric measurements are known to be very noisy and characterising the factors contributing to the noise are especially important before reliable scientific observations can be made. Majority of the work presented in this thesis concentrates on improving data processing of Doppler lidar systems.

The methods presented in **Papers I-II** were applied to a specific Doppler lidar system, which is briefly described below but, in principal, the methods in **Paper I** can be applied to data from other lidar instruments as well which exhibit similar features in their background signal. The ABL turbulence classification method presented in **Paper III** was developed to be applicable with any Doppler lidar system, which provides vertical and horizontal winds with sufficiently high temporal and vertical resolution. The data processing methods were created to be as generalized as possible. Hence, in **Paper IV** some of the methods developed in **Paper I** were applied to a different lidar system, the High Spectral Resolution Lidar (HSRL), which is also described below briefly.

Halo Photonics Stream Line Doppler lidar is a pulsed Doppler lidar system using heterodyne detection fibre–optic technology, and operates in the near–infrared spectral region at 1.5 µm (Pearson et al., 2009). The instrument is eye–safe due to it's low pulse energy coupled with high pulse repetition rate and is able to operate continuously and nearly maintenance–free for months. The operational parameters can be configured by the user, but usually the instrument operates at 30 m vertical and from 1 to 30 s integration times depending on the environment the instrument is operating at and has an effective range from about 100 m to about 10 km. There are three versions available: Stream Line, Stream Line Pro, and Stream Line XR (**Paper II**). The main difference between the first two are that the Pro–version is aimed for Arctic (or similar) deployments, where the instrument has to withstand temperatures reaching -40 °C. Data processing concepts are the same for all the Halo versions; however details of the implementation depend on the instrument specifications (See **Paper II**). The Stream Line and Stream Line XR have full hemispherical scanning capability, which allows even very low–level scans (Vakkari et al., 2015). The instrument provides radial velocity measurements and co–polarized (some versions also cross–polarized) backscattered signal intensity in terms of SNR. In the following sections the Halo Photonics

Stream Line Doppler lidar is referred simply as *Halo DL*, and the term *Doppler lidar* refers to Halo DL only, if not mentioned otherwise. In the introductory part of this thesis only the Stream Line Halo DL data was used, but for reasons of convenience. The methods discussed in the introductory part of this thesis are applicable for all of the Halo DL versions. For a more detailed description of the instrument reader is referred to (Pearson et al., 2009) and to **Papers I-II**.

High spectral resolution lidar (HSRL) is a United States Department of Energy funded Atmospheric Radiation Measurement (ARM) program's profiling lidar system (Eloranta, 2005; Goldsmith, 2016). In **Paper IV**, some of the data processing methodologies initially developed for the Halo DL in **Paper I** were applied to HSRL measurements taken during a campaign described in **Paper V**. The aim was to identify elevated aerosol layers (**Paper IV**). The HSRL is able to measure both backscatter and extinction profiles simultaneously from the same measurement, thus enabling absolute calibration at each range bin of the profile. Profiles of optical depth, depolarization are also available from the system. HSRL system is very sensitive lidar which is able to track the development and evolution of elevated aerosol layers. Please see Eloranta (2005) and Goldsmith (2016) for a more in–detail description of the HSRL system.

2.1 Doppler lidar data processing methodologies

This Section discusses the data processing methodologies developed in **Papers I-II** for correcting bias in the Halo DL background signal, which is required for estimating accurate radial velocity uncertainties. In this Section, both of the terms *signal* and the abbreviation *SNR* mean the Halo DL background signal, if not mentioned otherwise. Calculation of the unbiased air motion variance, as presented in **Paper III**, is discussed in Section 2.2. Once vertical extent of the turbulent mixing can be estimated robustly, it can be used to investigate the vertical structure of the turbulence withing the ABL. Methods for estimating coupling of the turbulence and identifying the dominant sources causing turbulence developed in **Paper III** are discussed in Section 2.3.

2.1.1 Cloud and aerosol filtering from noisy Doppler lidar signal

The ability to robustly discriminate between atmospheric and background signal in Doppler lidar data is essential for all lidar retrievals. In general, this can be done simply

by using a SNR threshold. Selection of such threshold is arbitrary but investigating a sufficiently long data set one can usually determine a value that gives satisfactory results in most cases. However, if the background noise floor is not completely flat due to features in the instrumental background signal, a SNR threshold has to be set so high that the data availability is significantly decreased. Especially at sites where the aerosol load is low and thus aerosol returns weak, the features in the background signal can cause bias greater than the atmospheric signal. **Papers I-II** describes such features that are present in the background signal of most of the Halo DL units, and **Paper II** gives more in–detail description on the causes of these features.

Detection of the bias from the Halo DL background signal requires aerosol and cloud, i.e. atmospheric signal to be filtered out first since the shape of the background has to be modeled accurately before it can be corrected. A simple SNR threshold method is unsuitable since the bias can change the shape of the SNR profile as a function of range. In the Halo DL measurements, biased SNR profile shape follows the 1^{st} or 2^{nd} degree polynomial (**Paper I**), or inverse exponential (**Paper II**). The shape imposed by the bias on the SNR profiles is not propagated to the variance of SNR, however.

It is also assumed that when signal is backscattered from atmospheric particles, the variance in SNR is significantly larger than variance of background noise only and hence the SNR variance can be used in discriminating atmospheric signal from noise. A dynamic threshold is searched for by first selecting reference windows from the range bins that are farthest from the instrument. Atmospheric signal is assumed to be obsolete in these range bins. Then, SNR variance within the reference windows is filtered iteratively by using an initial threshold and then increasing the threshold at each iteration until less than 1% of the variance in the reference windows are filtered. The variance based filtering captures most of the atmospheric signal but filters out some background signal as well. The intention is not to extract the atmospheric signal accurately but to make sure all of the atmospheric signal is filtered out.

Some of the atmospheric signal, though, remains usually as outliers in the filtered profiles and could cause significant errors in determining the shape of the background. Thus, an outlier removal method is applied to the remaining screened SNR profiles. The SNR profiles are modeled with robust bi–square weighted linear regression. The outliers are detected by using Cook's distance method (Cook, 1982; Hoaglin and Welsch, 1978). They are identified by constructing a hat matrix, which is then used for calculating so called leverage points. Together with the residuals of the bi–square weighted linear

regression fit, the leverage points are used to calculate the Cook's distance. Values in the SNR profiles pre–filtered using the dynamic variance based threshold, which have the highest Cook's distance, are then filtered out as atmospheric signal remnants. After removing the outliers, background only SNR remains. Although this method can be used to screen background signal in general, if there are no bias in the background signal or if it has been corrected, the simple SNR threshold method is sufficient and computationally more efficient.

2.1.2 Step–detection from noisy Doppler lidar signal

Bias in the Halo DL background signal was shown to change from one profile to another in **Paper I** as a step–change. Although the step–changes were found to occur after the instrument performs a background check periodically for determining instrumental noise, other more random step–changes were observed as well (**Papers I-II**). The Halo DL signal, where the atmospheric signal has been screened, is still quite noisy and the detection of step–changes in the signal is very challenging.

The method developed in **Paper I** is based on multilevel wavelet decomposition (e.g. Daubechies, 1992), where the steps are detected by using convolving the background signal with a suitably selected wavelet, a Haar wavelet in this case. The screened parts of the signal have to be filled first to produce a coherent background signal field required by the wavelet decomposition. This is done by fitting 1^{st} or 2^{nd} polynomials to the background signal or by using robust 2D interpolation. The wavelet decomposition is repeated selected number of times where approximation and detail coefficients are produced at each iteration and the approximation coefficients from previous iterations are used as an input in the next. The approximation coefficients, as the name suggests, hold the features of the original background signal but due to the nature of convolution, the features get smoother and smoother at each iteration. Detail coefficients, on the other hand, get their maximum value at the point where the selected wavelet function's and the background signal's patterns match the most. Eventually, the step–changes can be detected as peaks in the detail coefficients of the highest selected level (the last iteration) of the wavelet decomposition. For detecting the step–changes in the Halo DL background signal, the wavelet decomposition was applied to background signal at several range bins separately and the detail coefficients from the decomposition were then summed together. This makes the peaks in the detail coefficients more pronounced

and they can be detected with a standard peak detection method robustly.

2.2 Vertical velocity statistics unbiased by random noise

As mentioned earlier, Doppler lidars can measure the vertical velocity directly in vertical pointing mode. The variance of the vertical velocity can be used to estimate turbulent properties (O'Connor et al., 2010). However, the velocity variance (σ_v^2), which the Doppler lidar observes, is the sum of contributions from different sources that cause variation into the air motions (Frehlich et al., 1998), as given by O'Connor et al. (2010):

$$\sigma_v^2 = \sigma_w^2 + \sigma_e^2 + \sigma_d^2 \tag{3}$$

where σ_w^2 is the variance caused by air motions, σ_e^2 is the instrumental noise and σ_d^2 is the variance caused when terminal fall speeds of particles, which pass through the measurement volume, change from one sample to the next. In precipitation there is a wide range of potential terminal fall speeds hence the variation in the mean fall speed from sample to sample (σ_d^2) may be significant. In non–precipitating cases σ_d^2 can be assumed to be negligible and thus neglected (O'Connor et al., 2010). So, in order to measure turbulent mixing in aerosol and cloud, the noise contribution σ_e^2 has to be accounted for, which can be achieved by two different previously proposed methods:

A) estimating the radial Doppler velocity uncertainty $\langle\sigma_e\rangle$ with the method presented by Rye and Hardesty (1993), calculating its variance $\langle\sigma_e^2\rangle$, and using it as a good approximation for σ_e^2 (O'Connor et al., 2010), referred as the *O'Connor method* hereinafter,

B) using autocovariance methodology to estimate the contribution of σ_e^2 to the σ_v^2 (Lenschow et al., 2000), referred as the *Lenschow method* hereinafter.

Paper I shows that $\langle\sigma_e^2\rangle$ is proportional to the SNR and thus any error in the SNR calculation provided by the instrument will propagate into the turbulent properties if method A) is utilized for determining the σ_w^2. **Paper I** presents an automated background correction method for detecting and removing any bias in the SNR of the

Halo DL. **Paper II** builds upon this further by improving the background noise floor in the SNR of Halo DL.

Ensuring the retrieval of skewness and kurtosis is unbiased by noise is challenging for both of the methods. Also, there is no standard practise for using method B) for Doppler lidar data and it requires some assumptions to be made (Bonin et al., 2016). Thus, in **Paper III** a method presented by Rimoldini (2014), hereinafter the *Rimoldini method*, is applied for the first time to Doppler lidar measurements for calculating unbiased σ_w^2 directly from σ_v^2 and $\langle\sigma_e^2\rangle$.

Calculation of unbiased vertical velocity statistics, variance and skewness, are required for estimating turbulent properties (Lenschow et al., 2012), i.e. the TKE dissipation rate and turbulence coupling. In previous studies mostly the Lenschow method has been used when calculating unbiased statistics (e.g. Grund et al., 2001; Tucker et al., 2009; Schween et al., 2014; Bonin et al., 2016). On one hand, the advantage of applying the Rimoldini method, as done in **Paper III**, is that it does not require any assumptions to be made and it is computationally very cost–effective, unlike the Lenschow method. On the other hand, both the Rimoldini and the O'Connor methods utilize the estimated radial velocity uncertainties and thus any error in the uncertainty estimates will propagate to the unbiased statistics. The assumptions required for the Lenschow method are the selection of number of lags used in calculating autocovariance function, and the selection of line fitting method for extrapolating to the zeroth flag. The number of lags used should be selected so that the time scale still remains within the inertial subrange (MacCready, 1962) and that the frozen turbulence hypotheses is still valid (Taylor, 1935). Also, Lenschow method requires high temporal resolution from the Doppler lidar radial velocity measurements, which becomes a limiting factor for implementing the method at high latitudes and other locations where aerosol load is low and where longer integration times have to be used.

Figure 1 shows the vertical velocity unbiased variance in 30 min temporal resolution calculated with the Rimoldini, O'Connor, and Lenschow methods, and variance calculated by using a conventional method. An in–depth study, such as Bonin et al. (2016) conducted, but which used only the Lenschow method, would be required for comparing unbiased statistics calculation methods against a reference measurements from a 3D sonic anemometer placed on a mast at least 100 meters from the surface.

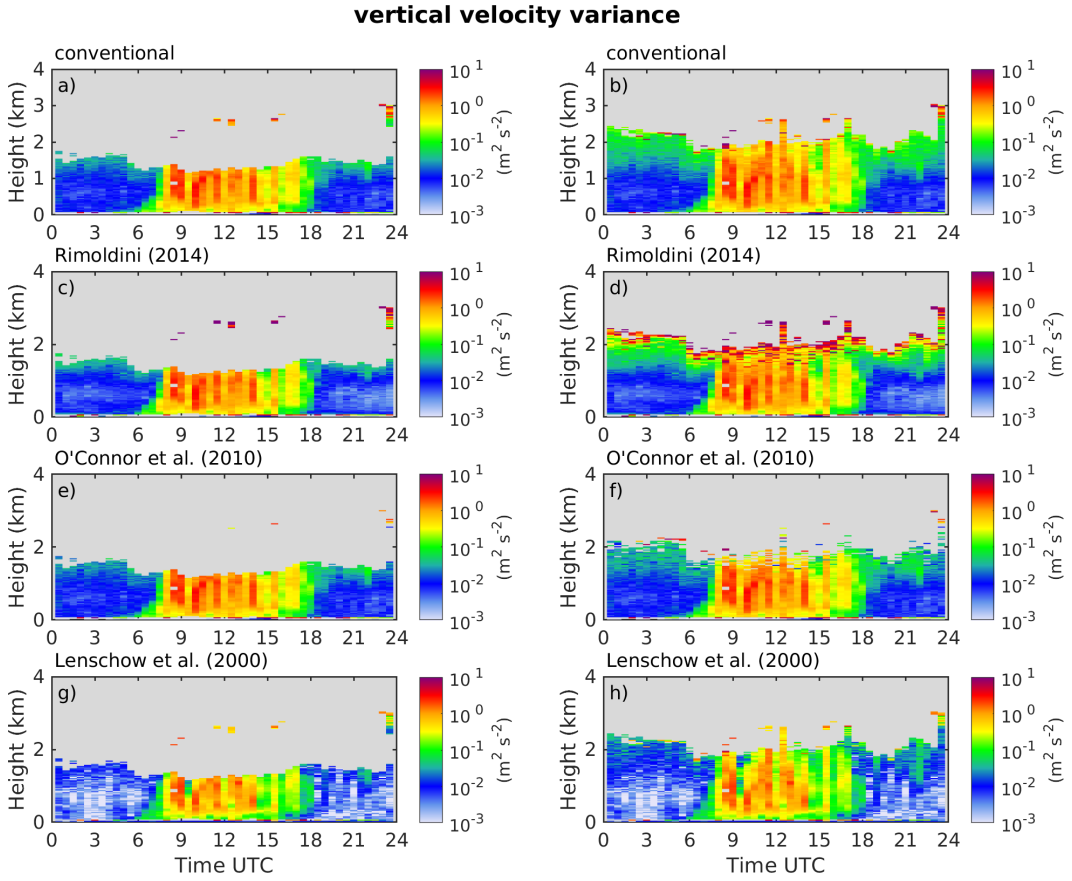

Figure 1: Time–height plots of vertical velocity variance measured with Halo DL on 17 July 2018 at Hyytiälä, Finland calculated by using a conventional method (a,b) and by using three methods presented by Rimoldini (2014), O'Connor et al. (2010), and Lenschow et al. (2000), which provide variance unbiased by noise (c-h). Two SNR thresholds, -23 db (a, c, e, g) and -28 dB (b, d, f, h), were used to illustrate their impact on data availability and highlight the differences in the performance of the methods at the top of the ABL where the SNR is generally low.

2.3 Bitfield generation

Bitfields are often used for example in satellite remote sensing to combine information from multiple measurements into one data field and to a scalar value in order to reduce the vast amount data retrieved by the satellite sensors. In **Paper III** several Halo DL quantities and supplementary data is combined into a bitfield, which withholds the information on the coupling of turbulence to the surface and/or clouds, and on the dominant sources causing turbulent mixing within the ABL. The Halo DL and supplementary quantities used in **Paper III** are converted into binary information (Table 1) by using threshold values:

$$\mathrm{bit}_n(t,r) = \begin{cases} 0 & \text{if } x(t,r) < a \\ 1 & \text{if } x(t,r) \geq a \end{cases},$$

where t is time, r is height above the ground level, x is the Halo DL quantity in question, a the respective threshold, and n is the number of the bit (Table 1). The ABL classification bitfield (B) is then generated by:

$$B(t,r) = \sum_{n=0}^{N-1} 2^n \mathrm{bit}_{n+1}(t,r), \tag{4}$$

where N is the total number of bits included into the ABL classification. In **Paper III** the bitfield is comprised of ten different bits each specifying a significance of a particular Doppler lidar or a supplementary quantity and hence the pixels in B can be, in principal, any scalar between 0 and 1024.

The thresholds in **Paper III** were taken from literature or found by experimentation (Fig 2). It is to be noted that selection of a threshold is always somewhat arbitrary. Even if a threshold value, which classifies a quantity as significant or insignificant and which works empirically in all locations and conditions, could be defined in theory, there are always noise in the data caused by various independent factors. For example, high vector wind shear can be observed during the daytime (Fig. 3). The high shear values mostly result from highly uncertain Doppler lidar winds retrieved in inhomogeneous wind field (Päschke et al., 2015; Vakkari et al., 2015; Newsom et al., 2017), and also the mechanical shear turbulence is assumed to be dominated by buoyancy driven turbulence

during the daytime (Oke, 1992). Figure 3e displays high vector wind shear values at about 500 m from 0:00 to about 6:00 UTC. No observable shear–driven turbulence can be observed though (Fig. 3e). Wind retrieval uncertainties increase significantly between 8:00 and 19:00 UTC when convection–driven turbulence disturbs laminar flow within the ABL and distorts the homogeneous wind field (Fig. 3b,d). Accordingly, the vector wind shear uncertainties, which are propagated from u– and v–wind components (**Paper III**), increase as well (Fig. 3f). Once the mixed layer erodes after about 18:00 UTC (Fig. 3g), wind shear (> 0.03 s^{-1}) generates turbulence near the surface below 500 m, which can be observed as high dissipation rate of TKE values ($> 10^{-4}$ m^2 s^{-3}).

As mentioned, the ABL classification bitfield contains large amount of information from the vertical structure of the ABL. The bitfield is used to generate masks illustrating turbulence coupling and the most dominant source causing turbulent mixing with high time and height resolution. The information held by the bitfield is combined by using a decision tree. In **Paper III**, a threshold–based approach was applied for its relatively simple and transparent logic. If additional measurements are available at some location, they can be added to the bitfield as a new bit (Eq. 4), and the decision tree can be updated easily.

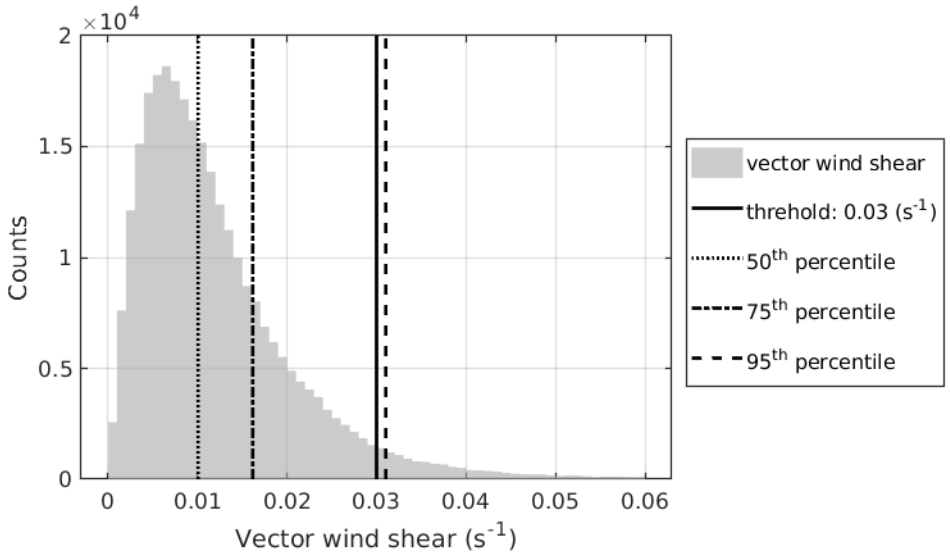

Figure 2: Histogram showing the distribution of vector wind shear values within the ABL and vertical lines depicting a selected threshold value for describing significance vector wind shear (solid), as well as the 50$^{\text{th}}$ (dotted), 75$^{\text{th}}$ (dash-dotted), and 95$^{\text{th}}$ (dashed) percentile values calculated from measurements during July 2015 at Jülich, Germany.

Table 1: Quantities used in generating the ABL classification bitfield

Bit number	Bit name / decision	Quantity / quantities used
1	Within ABL?	Backscatter signal
2	Turbulent?	Dissipation rate of TKE
3	Highly turbulent?	Dissipation rate of TKE
4	Coupled with the surface?	Dissipation rate of TKE & vertical velocity skewness
5	Unstable at surface level?	Sensible heat flux OR sunrise and sunset times
6	Wind shear?	Vector wind shear
7	In cloud?	Backscatter signal
8	Cloud–driven?	Backscatter signal & vertical velocity skewness
9	Convective?	Dissipation rate of TKE & vertical velocity skewness
10	Precipitating?	Vertical velocity & backscatter signal

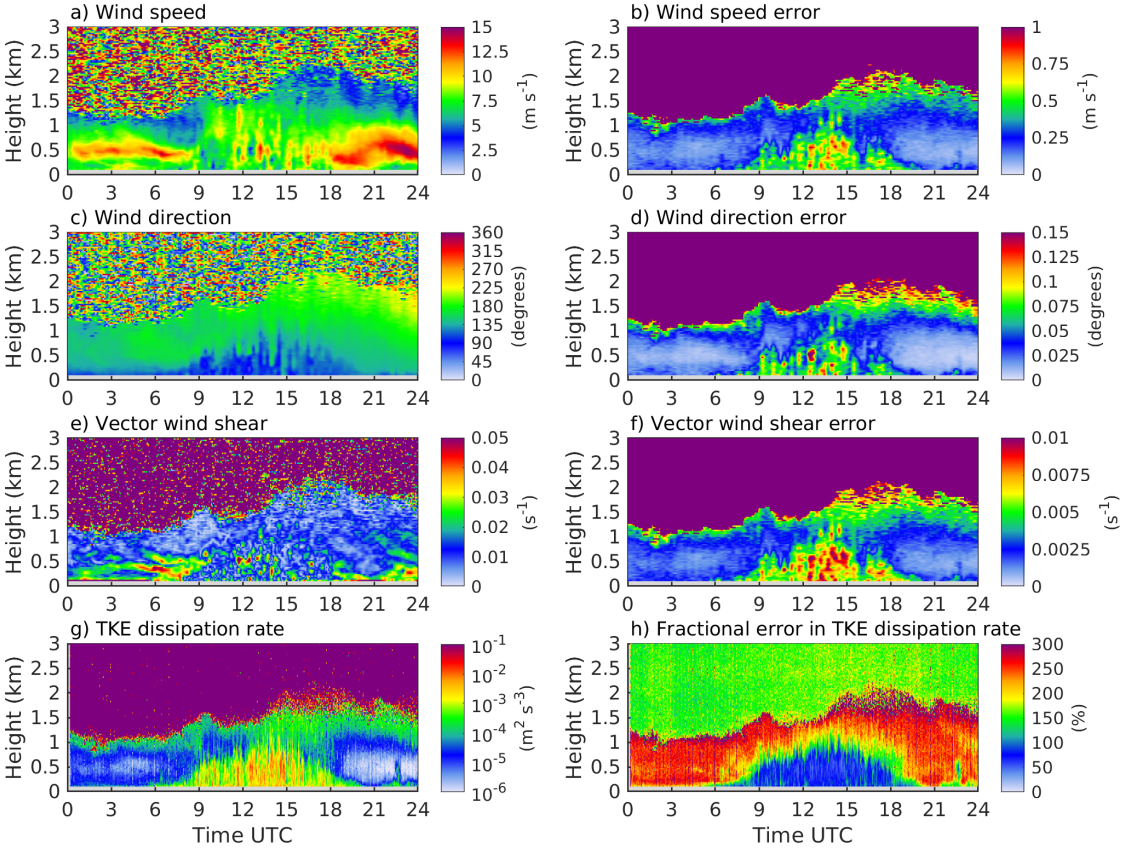

Figure 3: Time–height plots of wind speed (a), wind direction (c), vector wind shear (e), TKE dissipation rate (g), and their respective errors (b,d,f,h) calculated from Halo DL measurements on 31 July 2015 at Jülich, Germany.

3 Results and discussion

3.1 Improvements in Doppler lidar radial velocity uncertainties and sensitivity

The background features, i.e. varying bias in the Halo DL SNR, mentioned in Section 2.1.1 and described in–detail in **Papers I-II**, are clearly visible in Fig. 4a. The bias changes from one profile to the next which appear as step–changes in the time–height plots of the Halo DL signal. The step–changes propagate into the radial velocity uncertainties, as can be seen in Fig. 4c. Correcting the Halo DL signal with the background correction algorithm results to SNR field with effectively removed bias, if present, and to improved radial velocity uncertainties as can be seen in Fig. 4b,d. Notable also is the fact the lower the SNR, the higher the impact of the bias to signal and to radial velocity uncertainties, as can be seen in Fig. 4a at about 100 m above ground level (a.g.l.) from 11:00 to 13:00 UTC.

The background correction methods do not affect the radial velocities, but do affect the signal and thus the uncertainty of radial velocities since the uncertainties are proportional to the SNR (**Paper I**). Figure 4e-f shows a 2D histograms calculated from radial velocity and signal measured on 5 May 2017 at Hyytiälä, Finland. After the background correction, the noise floor is improved and centered at one in terms of SNR+1 (Fig. 4e-f) and is evenly distributed following a normal distribution (see **Paper II, Fig. A1**). This leads to higher data availability since after the correction the SNR threshold, which is used to determine between atmospheric signal and noise, can be set significantly lower than what has been previously suggested (Pearson et al. (2009): -17 dB, by Päschke et al. (2015): -20 dB) to about -22 dB, or to even -32 dB with the Halo XR system measurements (**Paper II**).

As mentioned earlier, at high latitude and other locations where the Halo DL SNR is generally low due to low aerosol load, longer integration times or averaging has to be used in order to improve the sensitivity. However, averaging cannot be done before correcting for the bias or features in the Halo DL background. It is generally assumed that when the noise is normally distributed the SNR can be improved by averaging the data and that the sensitivity improves by $1/\sqrt{\mathrm{N}}$, where N is the temporal averaging window (Δt). Figure 5 shows standard deviation of Halo DL SNR before (σ_{SNR_0}) and after (σ_{SNR_2}) the background correction presented in **Papers I-II**, one–

term power series fits, and the calculated theoretical σ_{SNR_0} and σ_{SNR_2} as a function of Δt = (0.5,1,2,...,29,30 min). If averaged before the correction the improvement in sensitivity is limited by the uncorrected noise floor (Fig. 6a,c,e). More precisely, the sensitivity is limited by the uncertainty in Halo DL *background*.txt* files, where the instrument stores periodical background checks (**Paper II**). After the correction the signal can be averaged and the sensitivity is significantly improved reaching nearly the theoretical limit (Fig 5).

Elevated aerosol layers become also distinguishable after the correction and averaging, and the height of the ABL can be estimated more accurately even when the SNR is low (from about 12:00 to 15:00 UTC at about 1500 m in Fig. 6). The background correction can also improve the Halo DL wind retrievals slightly. In addition to the increase in data availability, the more robust radial velocity uncertainties propagates into the uncertainty of wind retrievals (Päschke et al., 2015). Note, though, that there are other factors that also impact wind retrievals and their uncertainty (Newsom et al., 2017).

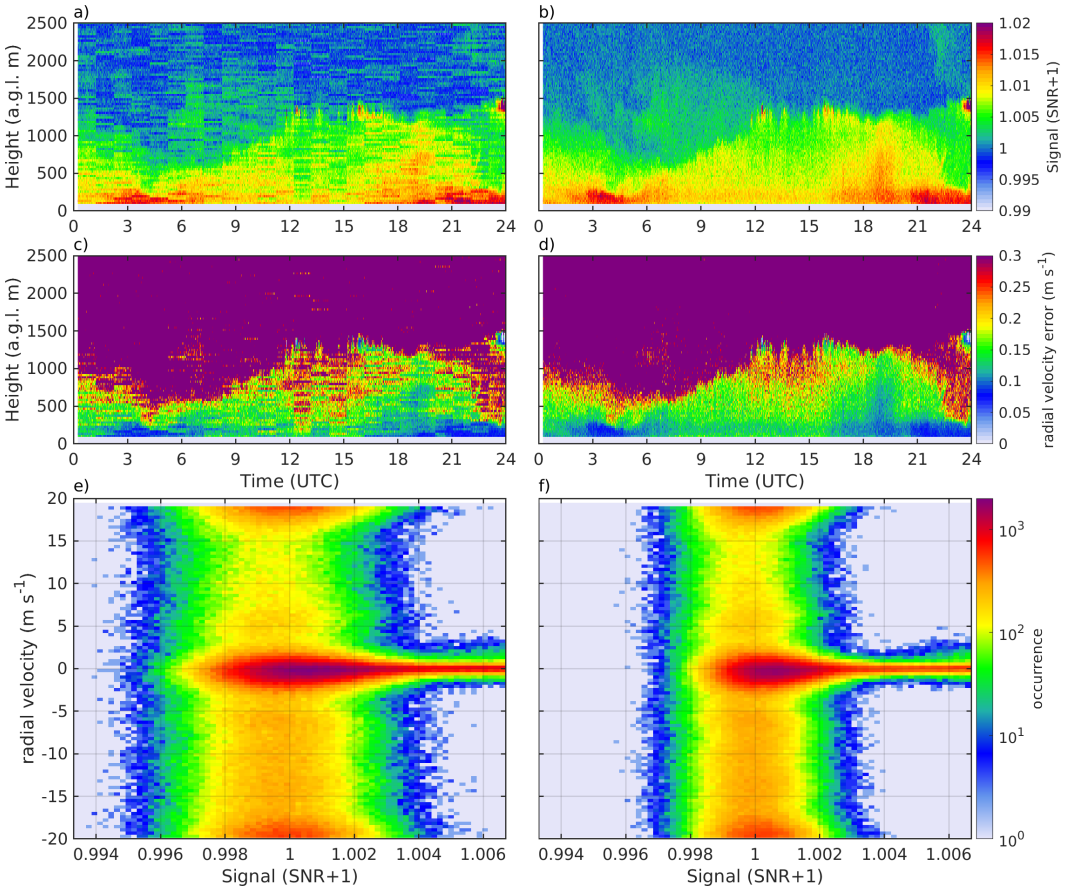

Figure 4: Time–height plots of signal (a-b) and radial velocity uncertainty estimates (c-d), and 2D–histogram plots calculated from radial velocity and signal (e-f) before (a,c,e) and after (b,d,f) the correction of the bias in SNR. Plotted measurement were taken on 5 May 2017 at Hyytiälä, Finland.

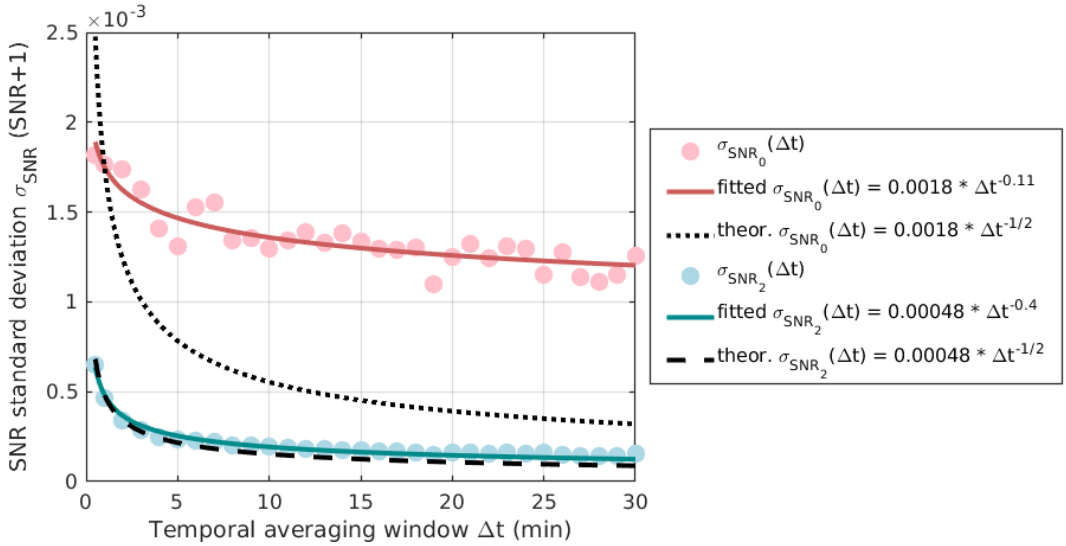

Figure 5: Standard deviation in Halo DL SNR before (σ_{SNR_0}) and after (σ_{SNR_2}) the background correction (following the notation in **Paper II**) calculated from a clear–sky period between two consecutive background checks from 1:00 and 2:00 UTC and data contained in range gates at about 3000m to 9600 m above ground level on 6 July 2015 at Jülich, Germany as a function of window length used in temporal averaging of the SNR (Δt). The solid lines represent the one–term power series fits ($f(\Delta\mathrm{t}) = a * \Delta\mathrm{t}^b$) for the σ_{SNR_0} and σ_{SNR_2}, and the dotted and dashed lines represent the theoretical values for the σ_{SNR_0} and σ_{SNR_2}, respectively, when assuming that the σ_{SNR} decreases, i.e. the sensitivity improves, by $1/\sqrt{\Delta\mathrm{t}}$.

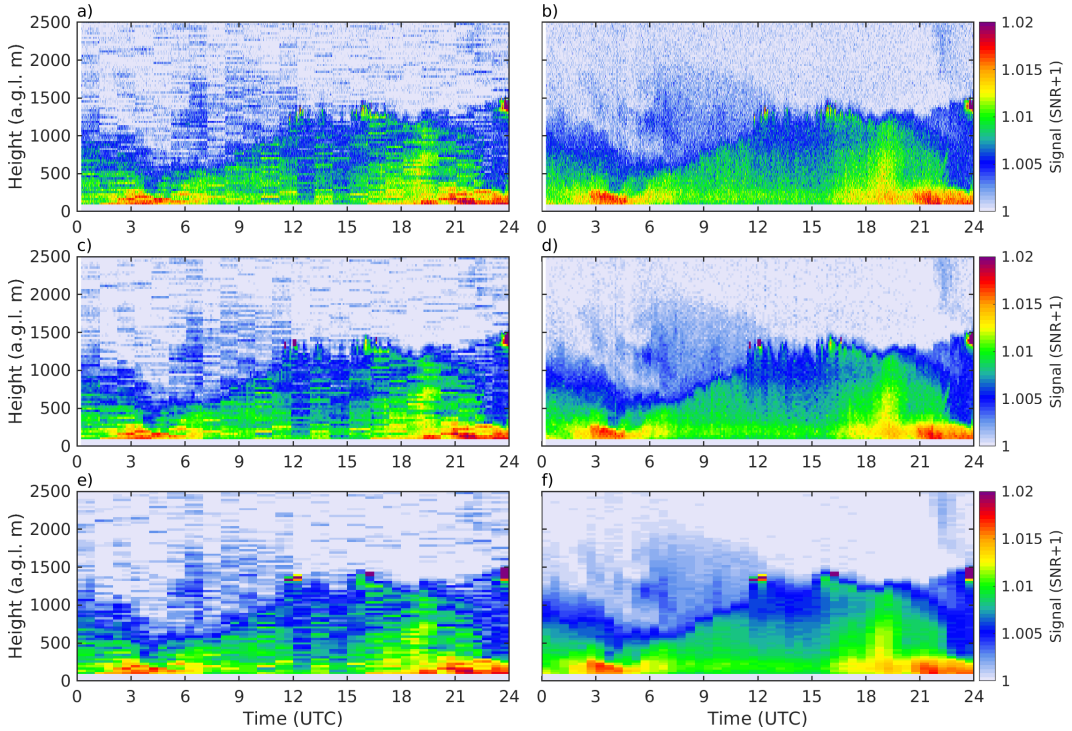

Figure 6: Time–height plots of signal before (a,c,e) and after (b,d,f) the background correction in original temporal resolution (a,b) and averaged to 3 minute (c,d) and to 30 minutes (e,f) temporal resolutions calculated from measurement taken on 5 May 2017 at Hyytiälä, Finland.

3.2 Atmospheric boundary layer classification with Doppler lidar

In **Paper III** the turbulent coupling and source classification methods were applied to one year long data sets from two different sites: a high latitude rural site in boreal environment at Hyytiälä, Finland, and a mid–latitude semi–rural continental site at Jülich, Germany. The methods were shown to perform successfully in clear–sky and cloud–top ABL conditions. In precipitating periods the contribution of varying droplet fall speeds in a measurement volume to the observed vertical velocities variance (and hence to turbulent properties as discussed in Section 2.2) should be taken into account. Such method does not exist yet, so the ABL classification method only detects precipitation and omits profiles containing any precipitation.

The ABL classification method enables capturing the development of the ABL throughout the day in–detail. Convective mixing periods and vertical extent of convective mixing can be detected and separated from turbulent mixing caused by other sources, such as wind shear and cloud–driven turbulence. Calculated sun rise and sun set times were used as an estimate for stable and unstable ABL conditions near the surface. One must keep in mind, though, that the ABL does not become unstable or stable immediately after the sun rise or sun set, respectively, and that for instance atmospheric conditions and local topography affect the time lag involved in the transformation between the atmospheric states.

Turbulent mixing can be, of course, caused by a mixture of sources, and thus the main product of the ABL classification method, the bitfield, holds information on all of the detected sources. Classification masks (**Paper III, Fig. 4, 6**) are derived from the bitfield by using a decision tree logic (**Paper III, Fig. 2**) and the masks present the detected dominating source for the turbulence. If auxiliary information is available, or methods for retrieving Doppler lidar quantities improve, the bitfield can be supplemented, the decision tree can be updated, and more classes can be added to the turbulent sources classification.

When applied to a suitably long data set, a climatology can be calculated from the ABL classification results and diurnal and seasonal cycle of turbulent mixing and vertical distribution can be studied. An example of such climatologies were presented in **Paper III** drawn from the one year long data set measured at the Hyytiälä and Jülich. Three different height ranges were selected in **Paper III**: 105-555 m, 585-1035 m, and 1065-

1515 m above ground level. Clear diurnal cycles of turbulent mixing were observed at both sites at the lowest height ranges. At the two highest height ranges diurnal cycles were apparent at Jülich, where as at Hyytiälä they were almost obsolete due to the difference in latitude. However, the most obvious difference between the sites, even after the background correction discussed in Section 2.1, was the data availability. Cloud presence at both sites was relatively high: about 30 % in winter and about 10 % in summer at Hyytiälä, and about 15 % in winter and about 10 % in summer at Jülich. Also, there was a significant contribution from cloud–driven turbulence, especially at Jülich, where also wind shear contributed to more than 10 % of the detected turbulent mixing during nighttime. The wind shear during nighttime was though to be caused by low–level jets, which was later investigated by Marke et al. (2018). At Hyytiälä, as expected, the ABL turbulent mixing was dominated by in–cloud turbulence due to the high cloud presence already at the lowest height range.

3.3 Identification of elevated aerosol layers from lidar measurements

In **Paper IV** the step–detection method developed in **Paper I** was applied to HSRL backscatter cross section and depolarisation profiles to detect elevated aerosol layers. The step–detection method was developed mainly to be used for detecting step–changes in Halo DL noise, as discussed earlier in Sect. 2.1.2, though, the method can be used also with other type of data with different noise characteristics. The method detects gradients in the data whose shape match well with the shape of the selected wavelet decomposition filter. HSRL noise has different characteristics than Halo DL noise, but elevated aerosol layers appear as step–changes in the HSRL backscatter and depolarisation profiles. The method was tested with two different case studies covering clear–sky and cloudy atmospheric conditions. The vertical structure of the ABL was simplified to six different layers identified from backscatter and depolarisation fields, where the first and the lowest layer was determined to comprised of the mixing layer and the residual layer.

The layer detection from the HSRL observations was verified with co–located radio sounding and airbourne in–situ aerosol measurements. Different layers can be observed clearly in the specific humidity profiles from radio soundings, where the specific humidity values within a well–mixed layer are apparently homogeneous. In all of the

cases the ABL was distinguished from elevated aerosol layers with the step–detection method. This was confirmed by significant differences between the ABL and the elevated layers in terms of aerosol number concentrations measured with the airbourne in–situ measurements.

3.4 Toolbox for processing Doppler lidar data

In order to address the gap in between the understanding of the ABL physics and their representation in high resolution climate and NWP models, *"creation of a catalogue of the more extensive ABL data sets"* (Baklanov and Grisogono, 2008) is required. Doppler lidars have been used extensively to study the ABL structure in various locations, but the studies have mainly concentrated on a few specific quantities from the site in question. Calculation of the same quantities from all of the sites is essential for cataloguing the ABL data sets. Thus, to harness the full capacity of the Doppler lidar, standardized methods should be applied to measurements from different sites to provide harmonized Doppler lidar retrievals.

Doppler lidars are being operated by several research groups at least in Europe and in Northern America, and often algorithms and software developed in–house are in use to process the Doppler lidar data. Research groups who are new to operating a Doppler lidar are often forced to develop their own software for handling the data. A collected catalogue of data sets from different research groups would then contain Doppler lidar retrievals generated with multiple different algorithms, different temporal and spatial resolutions, and possible discrepant uncertainties. Clearly there is need for a freely available software package to produce harmonized Doppler lidar retrievals with robust and consistent uncertainty estimates. This need led to the development of the Halo lidar toolbox, which is freely available from GitHub website (Manninen, 2019) and contains all the required steps to process the Halo DL measurements into Doppler lidar retrievals by using methods presented in peer–reviewed articles (Fig. 7), among the ones discussed in **Papers I-III**.

The toolbox was created initially for Halo DL, but in the future the aim is to expand the toolbox to encompass Doppler lidar systems from other manufacturers as well. In order to use the toolbox for processing Halo DL data the instrumental parameters have to be known and collected into a database where the software can access them when needed. Some of the parameters are instrument specific (Table 2) and some

are configurable by the user and are selected to suit the environment where Halo DL operates.

The toolbox is being actively developed and as of writing of this thesis, Table 3 lists all of the Doppler lidar quantities and products that the Halo lidar toolbox is able to generate. Error estimates, which are essential for climate and NWP model data assimilation, are provided for all of the quantities. The toolbox is intended to be site–independent so it can be used to generated from multiple sites and then catalogued together for model data assimilation purposes.

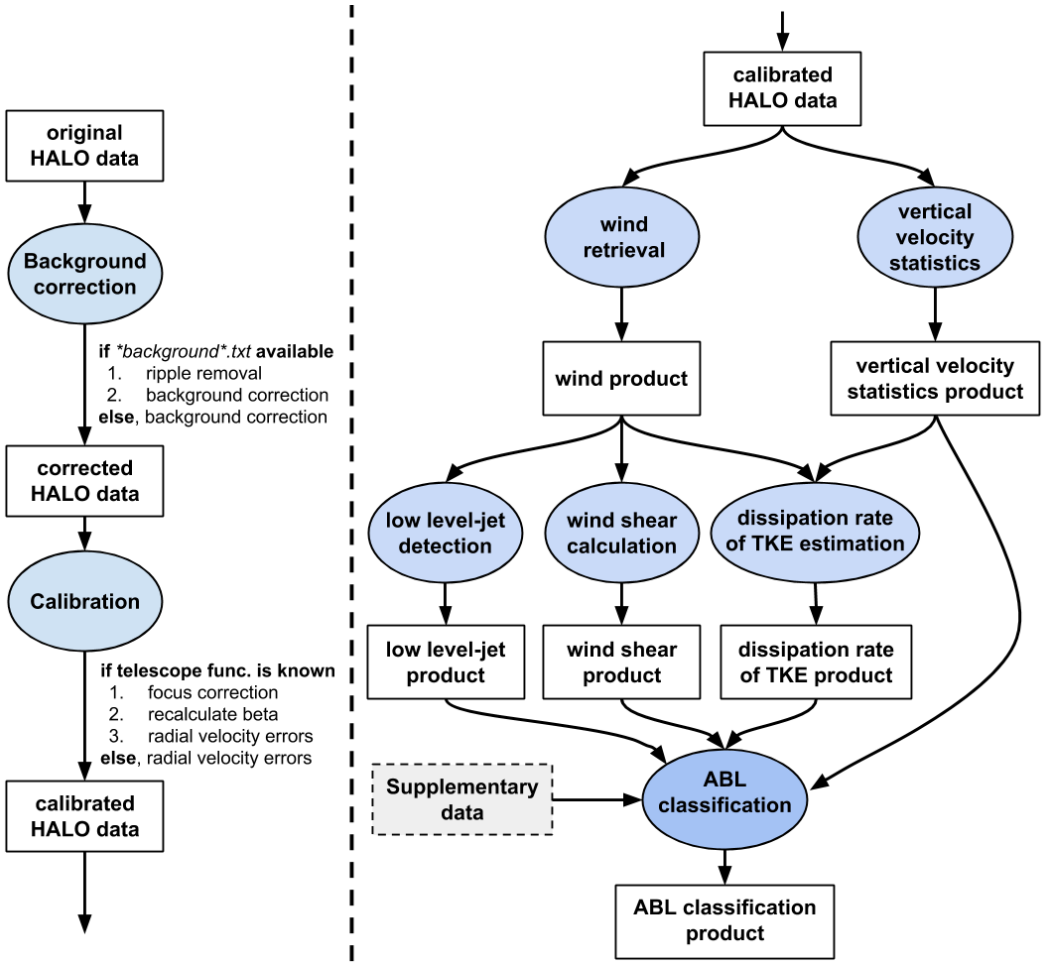

Figure 7: Sketch diagram of the Halo lidar toolbox processing chain illustrating the data processing steps from the original uncorrected data to the ABL classification product.

Table 2: Instrument specific parameters required by the Halo lidar toolbox

Parameter	Example (units)	Parameter	Example (units)
unit number	146	divergence	3.3e-5 (rad)
system	Halo Stream Line	number of lags	6
latitude	34.4567 (deg)	lens diameter	6e-2 (m)
longitude	12.2309 (deg)	energy	1e-5
altitude	34.5 (m agl)	wavelength	1.5e-6 (m)
focus range	65535 (m)	PRF*	15e3 (Hz)
number of pulses	15e3	pulse length	2e-7 (s)
samples per gate	10	sampling frequency	5e7 (Hz)
Nyquist velocity	19.456 (m s^{-1})	beam width	1.5e-4 (m)

*PRF = pulse repetition frequency

Table 3: Doppler lidar quantities and products produced by the Halo lidar toolbox

Doppler lidar product/quantity	Method published in
Background corrected SNR	**Paper I**, **Paper II**
Radial velocity uncertainties	Rye and Hardesty (1993), Pearson et al. (2009)
Wind speed and direction	Päschke et al. (2015), Newsom et al. (2017)
Vertical velocity statistics	O'Connor et al. (2010), Rimoldini (2014)
Dissipation rate of TKE	O'Connor et al. (2010)
Vector wind shear	ICAO (2005), **Paper III**
Low level-jet detection	Tuononen et al. (2017)
ABL classification	**Paper III**

4 Review of papers and author's contribution

Paper I presents a method for correcting features in the background noise of Halo Photonics Streamline Doppler lidars. The background noise features, which appear as step changes in the SNR time series and as a shape changes between consecutive SNR profiles, cause bias. After the bias is removed by the correction, SNR threshold, which determines the lowest limit for good atmospheric signal, can be set more than two decibels lower than before the correction. This, in turn, increases the data availability by as mush as 50 %. The correction also improves the turbulent property estimates since any bias in the SNR propagates in to the radial Doppler velocity uncertainties and to turbulent calculations. The algorithm was developed by me and I also wrote most of the paper.

Paper II presents a novel post-processing algorithm for the Halo Photonics Streamline Doppler lidars and improves the sensitivity of the instruments by factor of five or more. In addition to the background noise features described by the **Paper I**, the method improves the instrumental noise floor. After applying the algorithm, the background noise follows a normal distribution centered at 1 (SNR+1), and thus enables averaging existing high temporal resolution data or using a longer integration time for future measurements. The algorithm increases data availability significantly due to the improved noise floor, improves radial Doppler velocity uncertainty estimates and turbulent property retrievals. I helped in the algorithm development and contributed in writing of the paper.

Paper III describes a method to classify main source for causing turbulent mixing within the ABL. Classification can be done with standalone Doppler wind lidar measurements or together with complementary measurements, such as sensible heat flux, for example. The classification method and climatology derived from the classification enable investigation of the processes dominating the turbulent mixing with high time and height resolutions and provides information on the temporal and spatial variation of the turbulent mixing within the ABL, respectively. I did most of the coding for the algorithm, the method was developed together with Tobias Marke with whom we contributed equally to the writing of the paper.

Paper IV investigates elevated aerosol layers by combining airborne in-situ measurements, radio soundings, and ground based lidar profiles. Several case studies were chosen, elevated aerosol layers were detected from the HSRL profiles and from ra-

dio sounding, and co-located and coinciding airborne in-situ measurements were used to study the aerosol properties with the layers. I contributed in the flight campaign measurements and data collection, in HSRL data analysis, and in writing of the paper.

Paper V investigated the impact of biogenic aerosols on clouds and climate by combining a comprehensive array of ground based and airborne in–situ measurements of aerosol properties, and ground based remote sensing measurements for a 8-month long campaign. During the campaign I compared the in–situ campaign measurements of aerosol properties to the corresponding continuous measurements carried out at the SMEAR-II site and contributed to the writing of the paper.

5 Conclusions and future perspectives

The overarching topic of this thesis was to investigate what is needed for resolving the ABL vertical structure with continuous high temporal and vertical resolution, and can the dominating sources causing turbulent mixing be identified. The phenomena occurring within the ABL exhibit a wide range of temporal and spatial scales: from 1 second to one day, from meters to kilometres vertically, and up to 100 km horizontally which impose a great challenge for the measurements. In recent years, Doppler lidars have been shown to have distinctive advantage in measuring the ABL structure since they are able to operate continuously with very high time and height resolutions. Scanning Doppler lidars can provide also wind profile and can be used to investigate how representative the vertical profile measurements are horizontally. Although, Doppler lidars have been used to monitor the ABL continuously at various locations, some notable limitations remain in very low SNR clean–air conditions. **Papers I-II** present methods for Halo Photonics Streamline Doppler lidar to overcome these limitations and significantly improve the sensitivity of the instrument. **Paper III** describes a site–independent classification method for identifying main sources causing turbulent mixing with Doppler wind lidar, **Paper IV** investigates vertical structure of ABL, especially elevated aerosol layers, and **Paper V** discusses the advantages of investigating the ABL phenomena and structure by using multi–instrument approach.

Paper I describes an algorithm for correcting bias in the Halo Doppler lidar measurements. To be able to retrieve turbulent properties from Doppler lidar measurements, and to investigate the distribution of turbulence within the ABL, the radial Doppler velocity uncertainties have to be estimated robustly. However, any bias in the SNR propagates into the radial Doppler velocity uncertainties and further into turbulent properties. Further, in **Paper II** the performance of the Halo Doppler lidar is significantly improved by identifying and correcting deviations in instrumental noise floor, and thus increasing sensitivity by several factors. It is to be noted, that any improvements to the Halo Doppler lidar SNR gained by averaging or by using a longer integration time can be achieved only after any biases and/or the background noise floor has been corrected. Data availability is increased dramatically at high latitude or other clean-air locations because the SNR threshold used to determine atmospheric signal from background can be set much lower after the corrections. The improved sensitivity also enables investigation of cirrus clouds and elevated aerosol layers, which has previously been thought as out of scope of the instrument.

After the corrections, the Halo Doppler lidar measurements can be used for retrieving turbulent properties and other quantities, such as vector wind shear and vertical velocity skewness. **Paper III** describes a scheme which combines these retrievals and, if available, complementary measurements and identifies the dominant sources causing turbulent mixing within the ABL. The site–independent method can discriminate between buoyancy and mechanical friction driven turbulent mixing and is it connected to the surface, to clouds, or neither. The main outcome is a classification bitfield, where each bit contains information on the retrieved lidar and complimentary quantities. The bitfield is given in time—height dimensions with highest temporal and vertical resolutions of 3 minutes and 30 meters (depending on instrument parameters), respectively. Two classification masks can be produced from the bitfield: 1) presences of turbulent mixing and its association to clouds, surface or neither, and 2) identified dominant sources for turbulent mixing. These fields will provide information with high temporal and vertical resolution on the vertical structure of turbulence within the ABL. A climatology describing vertically resolved diurnal and seasonal cycles of turbulent mixing can be derived by applying the ABL classification scheme to sufficiently long data set.

The developed data processing methodologies were applied to profiling HSRL lidar measurements as well. In **Paper IV** a step–change detection method based on wavelet decomposition, which was presented in **Paper I**, was successfully used to detect elevated aerosol layers. Several separate layers were identified and elevated layers were discriminated from the ABL. Layer separation together with co–located and coincident airborne in–situ, and radio sounding measurements enabled in–detail investigation of aerosol properties in each separate layer and their vertical distribution of aerosols, which is essential for direct and indirect radiative forcing studies.

Doppler lidars, like many remote sensing instruments, output an immense amount of data which can be processed into multiple stand–alone scientific observations and data products. In order to reliably compare observations from different sites and environments, the data products must be harmonized and be generated with the same, preferably, peer–reviewed methods. At the time of writing this thesis, the Halo lidar toolbox has been tested already at several sites and has been used to collect ABL data sets and climatologies. These data sets reveal essential information on the vertical transport within the ABL. Though, to fully reveal the ever developing ABL structure and atmosphere–surface exchanges, a holistic multi–instrument synergy approach is required, such as described e.g. by **Paper V**, and preferably be carried out con-

tinuously where co–located measurements can be processed into synergetic scientific observations.

References

American Meteorological Society (2019a). Glossary of Meteorology: Atmospheric boundary layer.

American Meteorological Society (2019b). Glossary of Meteorology: Mixed layer.

Anderson, J. O., Thundiyil, J. G., and Stolbach, A. (2012). Clearing the Air: A Review of the Effects of Particulate Matter Air Pollution on Human Health. *Journal of Medical Toxicology*, 8(2):166–175.

Baars, H., Ansmann, A., Engelmann, R., and Althausen, D. (2008). Continuous monitoring of the boundary-layer top with lidar. *Atmospheric Chemistry and Physics Discussions*, 8(3):10749–10790.

Baklanov, A. and Grisogono, B. (2008). Atmospheric boundary layers: nature, theory and applications to environmental modelling and security. In Baklanov, A. and Grisogono, B., editors, *Atmospheric Boundary Layers*, pages 1–4. Springer New York, New York, NY.

Baklanov, A. A., Grisogono, B., Bornstein, R., Mahrt, L., Zilitinkevich, S. S., Taylor, P., Larsen, S. E., Rotach, M. W., and Fernando, H. J. S. (2011). The Nature, Theory, and Modeling of Atmospheric Planetary Boundary Layers. *Bulletin of the American Meteorological Society*, 92(2):123–128.

Bonin, T. A., Carroll, B. J., Hardesty, R. M., Brewer, W. A., Hajny, K., Salmon, O. E., and Shepson, P. B. (2018). Doppler Lidar Observations of the Mixing Height in Indianapolis Using an Automated Composite Fuzzy Logic Approach. *Journal of Atmospheric and Oceanic Technology*, 35(3):473–490.

Bonin, T. A., Choukulkar, A., Brewer, W. A., Sandberg, S. P., Weickmann, A. M., Pichugina, Y. L., Banta, R. M., Oncley, S. P., and Wolfe, D. E. (2017). Evaluation of turbulence measurement techniques from a single Doppler lidar. *Atmospheric Measurement Techniques*, 10(8):3021–3039.

Bonin, T. A., Newman, J. F., Klein, P. M., Chilson, P. B., and Wharton, S. (2016). Improvement of vertical velocity statistics measured by a Doppler lidar through comparison with sonic anemometer observations. *Atmospheric Measurement Techniques*, 9(12):5833–5852.

Borque, P., Luke, E., and Kollias, P. (2016). On the unified estimation of turbulence eddy dissipation rate using Doppler cloud radars and lidars: Radar and Lidar Turbulence Estimation. *Journal of Geophysical Research: Atmospheres*, 121(10):5972–5989.

Bhl, J., Leinweber, R., Grsdorf, U., Radenz, M., Ansmann, A., and Lehmann, V. (2015). Combined vertical-velocity observations with Doppler lidar, cloud radar and wind profiler. *Atmospheric Measurement Techniques*, 8(8):3527–3536.

Cohen, A. E., Cavallo, S. M., Coniglio, M. C., and Brooks, H. E. (2015). A Review of Planetary Boundary Layer Parameterization Schemes and Their Sensitivity in Simulating Southeastern U.S. Cold Season Severe Weather Environments. *Weather and Forecasting*, 30(3):591–612.

Cook, R. D. (1982). *Residuals and influence in regression*. Chapman & Hall, New York, NY.

Daubechies, I. (1992). *Ten Lectures On Wavelets*, volume 61 of *CBMS-NSF Regional Conference Series in Applied Mathematics*. Society for Industrial and Applied Mathematics, 8th edition.

Deardorff, J. W. (1972). Numerical Investigation of Neutral and Unstable Planetary Boundary Layers. *Journal of the Atmospheric Sciences*, 29(1):91–115.

Eloranta, E. W. (2005). High Spectral Resolution Lidar. In Weitkamp, C., editor, *LIDAR: range-resolved optical remote sensing of the atmosphere*. Springler-Verlag, New York, NY.

Engelbart, D. A., Kallistratova, M., and Kouznetsov, R. (2007). Determination of the turbulent fluxes of heat and momentum in the ABL by ground-based remote-sensing techniques (a Review). *Meteorologische Zeitschrift*, 16(4):325–335.

ESA (2008). ADM-Aeolus Science Report. Technical Report SP-1311, European Space Agency ESA, Noordwijk, The Netherlands.

Frehlich, R., Hannon, S. M., and Henderson, S. W. (1998). Coherent Doppler Lidar Measurements of Wind Field Statistics. *Boundary-Layer Meteorology*, 86(2):233–256.

Garratt, J. (1994). Review: the atmospheric boundary layer. *Earth-Science Reviews*, 37(1-2):89–134.

Goldsmith, J. (2016). High Spectral Resolution Lidar (HSRL) Instrument Handbook. Technical Report DOE/SC-ARM-TR–157, 1251392.

Grund, C., Banta, R., George, J., Howell, J., Post, M., Richter, R., and Weickmann, A. (2001). High-Resolution Doppler Lidar for Boundary Layer and Cloud Research. *Journal of Atmospheric and Oceanic Technology*, 18(3):376–393.

Harvey, N. J., Hogan, R. J., and Dacre, H. F. (2013). A method to diagnose boundary-layer type using Doppler lidar: A Method to Diagnose Boundary-Layer Type. *Quarterly Journal of the Royal Meteorological Society*, 139(676):1681–1693.

Harvey, N. J., Hogan, R. J., and Dacre, H. F. (2015). Evaluation of boundary-layer type in a weather forecast model utilizing long-term Doppler lidar observations: Evaluation of Boundary-Layer Type Forecasts. *Quarterly Journal of the Royal Meteorological Society*, 141(689):1345–1353.

Hirsikko, A., O'Connor, E. J., Komppula, M., Korhonen, K., Pfller, A., Giannakaki, E., Wood, C. R., Bauer-Pfundstein, M., Poikonen, A., Karppinen, T., Lonka, H., Kurri, M., Heinonen, J., Moisseev, D., Asmi, E., Aaltonen, V., Nordbo, A., Rodriguez, E., Lihavainen, H., Laaksonen, A., Lehtinen, K. E. J., Laurila, T., Petäjä, T., Kulmala, M., and Viisanen, Y. (2014). Observing wind, aerosol particles, cloud and precipitation: Finland's new ground-based remote-sensing network. *Atmospheric Measurement Techniques*, 7(5):1351–1375.

Hoaglin, D. C. and Welsch, R. E. (1978). The Hat Matrix in Regression and ANOVA. *The American Statistician*, 32(1):17–22.

Hogan, R. J., Grant, A. L. M., Illingworth, A. J., Pearson, G. N., and O'Connor, E. J. (2009). Vertical velocity variance and skewness in clear and cloud-topped boundary layers as revealed by Doppler lidar. *Quarterly Journal of the Royal Meteorological Society*, 135(640):635–643.

Holtslag, A. A. M., Svensson, G., Baas, P., Basu, S., Beare, B., Beljaars, A. C. M., Bosveld, F. C., Cuxart, J., Lindvall, J., Steeneveld, G. J., Tjernstrm, M., and Van De Wiel, B. J. H. (2013). Stable Atmospheric Boundary Layers and Diurnal Cycles: Challenges for Weather and Climate Models. *Bulletin of the American Meteorological Society*, 94(11):1691–1706.

ICAO (2005). Manual on Low-level Wind Shear. Technical report, International Civil Aviation Organization.

Lenschow, D. H., Lothon, M., Mayor, S. D., Sullivan, P. P., and Canut, G. (2012). A Comparison of Higher-Order Vertical Velocity Moments in the Convective Boundary Layer from Lidar with In Situ Measurements and Large-Eddy Simulation. *Boundary-Layer Meteorology*, 143(1):107–123.

Lenschow, D. H., Wulfmeyer, V., and Senff, C. (2000). Measuring Second- through Fourth-Order Moments in Noisy Data. *Journal of Atmospheric and Oceanic Technology*, 17(10):1330–1347.

MacCready, P. B. (1962). The inertial subrange of atmospheric turbulence. *Journal of Geophysical Research*, 67(3):1051–1059.

Manninen, A. J. (2019). Halo lidar toolbox, GitHub, available at: https://github.com/manninenaj/HALO_lidar_toolbox (last access: 26 February 2019).

Marke, T., Crewell, S., Schemann, V., Schween, J. H., and Tuononen, M. (2018). Long-Term Observations and High-Resolution Modeling of Midlatitude Nocturnal Boundary Layer Processes Connected to Low-Level Jets. *Journal of Applied Meteorology and Climatology*, 57(5):1155–1170.

Moeng, C.-H. and Sullivan, P. P. (1994). A Comparison of Shear- and Buoyancy-Driven Planetary Boundary Layer Flows. *Journal of the Atmospheric Sciences*, 51(7):999–1022.

Newsom, R. K., Brewer, W. A., Wilczak, J. M., Wolfe, D. E., Oncley, S. P., and Lundquist, J. K. (2017). Validating precision estimates in horizontal wind measurements from a Doppler lidar. *Atmospheric Measurement Techniques*, 10(3):1229–1240.

Nielsen-Gammon, J. W., Hu, X.-M., Zhang, F., and Pleim, J. E. (2010). Evaluation of Planetary Boundary Layer Scheme Sensitivities for the Purpose of Parameter Estimation. *Monthly Weather Review*, 138(9):3400–3417.

Oke, T. R. (1992). *Boundary layer climates*. Routledge, London; New York, 2nd edition.

O'Connor, E. J., Illingworth, A. J., Brooks, I. M., Westbrook, C. D., Hogan, R. J., Davies, F., and Brooks, B. J. (2010). A Method for Estimating the Turbulent Kinetic Energy Dissipation Rate from a Vertically Pointing Doppler Lidar, and Independent

Evaluation from Balloon-Borne In Situ Measurements. *Journal of Atmospheric and Oceanic Technology*, 27(10):1652–1664.

Pearson, G., Davies, F., and Collier, C. (2009). An Analysis of the Performance of the UFAM Pulsed Doppler Lidar for Observing the Boundary Layer. *Journal of Atmospheric and Oceanic Technology*, 26(2):240–250.

Päschke, E., Leinweber, R., and Lehmann, V. (2015). An assessment of the performance of a 1.5mu Doppler lidar for operational vertical wind profiling based on a 1-year trial. *Atmospheric Measurement Techniques*, 8(6):2251–2266.

Reitebuch, O. (2012). Wind Lidar for Atmospheric Research. In Schumann, U., editor, *Atmospheric Physics, Research Topics in Aerospace*. Springer, Berlin.

Rimoldini, L. (2014). Weighted skewness and kurtosis unbiased by sample size and Gaussian uncertainties. *Astronomy and Computing*, 5:1–8.

Rye, B. J. and Hardesty, R. M. (1993). Discrete spectral peak estimation in incoherent backscatter heterodyne lidar. I. Spectral accumulation and the Cramer-Rao lower bound. *Geoscience and Remote Sensing, IEEE Transactions on*, 31(1):16–27.

Schobesberger, S., Väänänen, R., Leino, K., Virkkula, A., Backman, J., Pohja, T., Siivola, E., Franchin, A., Mikkilä, J., Paramonov, M., Aalto, P., Krejci, R., Petäjä, T., and Kulmala, M. (2013). Airborne measurements over the boreal forest of southern Finland during new particle formation events in 2009 and 2010. *Boreal Environment Research*, 18:145–163.

Schween, J. H., Hirsikko, A., Lhnert, U., and Crewell, S. (2014). Mixing-layer height retrieval with ceilometer and Doppler lidar: from case studies to long-term assessment. *Atmospheric Measurement Techniques*, 7(11):3685–3704.

Schwiesow, R. L., Kpp, P., and Werner, C. (1985). Comparison of CW-Lidar-Measured Wind Values Obtained by Full Conical Scan, Conical Sector Scan and Two-Point Techniques. *Journal of Atmospheric and Oceanic Technology*, 2(1):3–14.

Sonnenschein, C. M. and Horrigan, F. A. (1971). Signal-to-Noise Relationships for Coaxial Systems that Heterodyne Backscatter from the Atmosphere. *Applied Optics*, 10(7):1600.

Stull, R. B. (1988). *An Introduction to Boundary Layer Meteorology*. Springer Netherlands, Dordrecht.

Taylor, G. I. (1935). Statistical Theory of Turbulence. *Proceedings of the Royal Society of London. Series A - Mathematical and Physical Sciences*, 151(873):421–444.

Tucker, S. C., Senff, C. J., Weickmann, A. M., Brewer, W. A., Banta, R. M., Sandberg, S. P., Law, D. C., and Hardesty, R. M. (2009). Doppler Lidar Estimation of Mixing Height Using Turbulence, Shear, and Aerosol Profiles. *Journal of Atmospheric and Oceanic Technology*, 26(4):673–688.

Tuononen, M., O'Connor, E. J., Sinclair, V. A., and Vakkari, V. (2017). Low-Level Jets over Ut, Finland, Based on Doppler Lidar Observations. *Journal of Applied Meteorology and Climatology*, 56(9):2577–2594.

Turner, D. D., Goldsmith, J. E. M., and Ferrare, R. A. (2016). Development and Applications of the ARM Raman Lidar. *Meteorological Monographs*, 57:18.1–18.15.

Vakkari, V., O'Connor, E. J., Nisantzi, A., Mamouri, R. E., and Hadjimitsis, D. G. (2015). Low-level mixing height detection in coastal locations with a scanning Doppler lidar. *Atmospheric Measurement Techniques*, 8(4):1875–1885.

Werner, C., Streicher, J., Leike, I., and Mnkel, C. (2005). Visibility and cloud lidar. In *LIDAR: range-resolved optical remote sensing of the atmosphere*. Springer, Berlin.

World Meteorological Organization (2018). Statement of Guidance for High Resolution Numerical Weather Prediction (NWP). Technical report.